International Journal of Biological Macromolecules 277 (2024) 133986

Contents lists available at ScienceDirect

International Journal of Biological Macromolecules

journal homepage: www.elsevier.com/locate/ijbiomac

Digested galactoglucomannan mitigates oxidative stress in human cells, restores gut bacterial diversity, and provides chemopreventive protection against colon cancer in rats

Amanda dos Santos Lima [a], Fernanda Rafaelly de Oliveira Pedreira [a], Nathália Alves Bento [a], Rômulo Dias Novaes [b], Elda Gonçalves dos Santos [b], Graziela Domingues de Almeida Lima [b], Leonardo Augusto de Almeida [c], Thiago Caetano Andrade Belo [c], Fernando Vitor Vieira [a], Nima Mohammadi [d], Petri Kilpeläinen [e], Alexandre Giusti-Paiva [f], Daniel Granato [d,*], Luciana Azevedo [a,*]

[a] *In vitro and in vivo Nutritional and Toxicological Analysis Lab, Federal University of Alfenas, Alfenas, Minas Gerais, Brazil*
[b] *Institute of Biomedical Sciences, Department of Structural Biology, Federal University of Alfenas, Alfenas, Minas Gerais, Brazil*
[c] *Department of Microbiology and Immunology, Federal University of Alfenas, Alfenas, Minas Gerais, Brazil*
[d] *Bioactivity & Applications Lab, Department of Biological Sciences, Faculty of Science and Engineering, School of Natural Sciences, University of Limerick, V94 T9PX Limerick, Ireland*
[e] *Biorefinery and Bioproducts, Production Systems Unit, Natural Resources Institute Finland (Luke), Myllytie 1, 31600 Jokioinen, Finland*
[f] *Center of Biological Sciences, Federal University of Santa Catarina, Florianópolis, Santa Catarina, Brazil*

ARTICLE INFO

Keywords:
Bioaccessibility
Hemicellulose
Erythrocytes

ABSTRACT

Galactoglucomannan (GGM) is the predominant hemicellulose in coniferous trees, such as Norway spruce, and has been used as a multipurpose emulsifier in the food industry. *In vitro* digestion with a cellular antioxidant activity assay was performed to determine the bioaccessibility and antioxidant activity of phenolic compounds, and the behaviour of GGM on *in vivo* experimental assay against induced colon cancer. The results showed that digestion decreased the bioaccessibility and antioxidant capacity of phenolic compounds. Cellular analysis did not support these findings once an antioxidant effect was observed in human cell lines. GGM attenuated the initiation and progression of colon cancer, by reducing the foci of aberrant crypts in rats, and modified the intestinal bacterial microbiota (disrupting the balance between Firmicutes and Bacteroidetes phyla). Thus, GGM provided chemopreventive protection against the development of colon cancer and acted as an intracellular antioxidant agent.

1. Introduction

The bark of coniferous trees is a by-product of the wood-processing industry. Because of its low, inexistent almost non-existent commercial value, tree bark is typically discarded without extracting valuable compounds, such as polysaccharides and polyphenols [1]. Tree bark contains various polysaccharides, mostly hemicelluloses and polyphenols, which are considered beneficial of health. However, it remains an industrial by-product that has not been extensively explored in the pulp and paper industry [2]. A new trend for extracting hemicelluloses from renewable biomass and available industrial by-products at low cost that can be used as value-added ingredients is promising [3].

Galactoglucomannans (GGM) are the main type of hemicellulose in softwoods (*i.e.*, spruce). They are classified as dietary fibre and consist of chiefly by 55–60 % mannose and 14–15 % glucose units, linked through β-(1 → 4) glycosidic linkages [4,5]. Research studies have shown show that GGM is a high-value-added material for techno-functional applications, as well as thickening and stabilising agents, film-forming agents, hydrogels, aerogels, which makes it a functional ingredient. These techno-functional properties are of industrial interest for food, cosmetics, and pharmaceutical applications [5,6].

Recent studies have shown that GGM affects cell proliferation, angiogenesis, and inflammation, inducing apoptosis and cell cycle arrest [1,7]. Furthermore, aqueous extracts rich in GGM have health-

* Corresponding authors.
E-mail addresses: Daniel.Granato@ul.ie (D. Granato), luciana.azevedo@unifal-mg.edu.br (L. Azevedo).

https://doi.org/10.1016/j.ijbiomac.2024.133986
Received 20 March 2024; Received in revised form 11 July 2024; Accepted 16 July 2024
Available online 20 July 2024

promoting effects and, act as therapeutic agents to prevent and treat symptoms of lower urinary tract inflammation [8]. Owing to these different biological activities, the valorisation of by-products can be attractive for the food industry to obtain nutritional and functional ingredients.

Despite these numerous potential benefits, studies on the antioxidant and anticarcinogenic effects of GGM extracts *in vitro* and *in vivo* are lacking, particularly regarding the analysis of this digested matrix using erythrocytes as a cell model. Simulated *in vitro* gastrointestinal digestion, although considered a static model, attempts to imitate the conditions expected *in vivo* to provide greater safety for use in animal tests [9]. The gastrointestinal tract can also promote changes in the profile and content of these compounds, affecting their bioavailability during intestinal absorption, mainly through the action of digestive enzymes and changes in pH [4].

Knowledge of the toxicological safety and bioactivity of new extracts from non-conventional sources is necessary so that renewable resources such as hemicelluloses in sawdust and softwood chips, can be more valued and better used [3]. GGM could be potentially used as a soluble dietary fibre, similar to guar gum and other galactomannans that resist hydrolytic digestion and are fermented in the large intestine. As a fermentable carbohydrate, the consumption of GGM could support gut health [10] and a reduction in the risk of colorectal cancer [11], which is one of the three types of cancer with the highest worldwide incidence (10.2 %) [12].

To fill this gap in the literature, the main objectives of this study were to characterise GGM extracts from Norway spruce bark by polyphenol determination and chemical antioxidant capacity screening, considering the chemical transformations caused by an *in vitro* digestion model. In addition, we investigated the biological potential and safety of GGM using *in vitro* analysis in human cell lines and investigated the modulation of microbiota and protection against precancerous lesions in rats with 1,2-dimethylhydrazine (DMH)-induced colorectal cancer.

2. Materials and methods

2.1. Galactoglucomannan (GGM): extraction and spray-drying

The GGM was obtained from Norway spruce (*Picea abies*) wood sawdust, collected in central and southern Finland, and stored at −20 °C. For the extraction process, a flow extractor (PHEW) was used with pressurised hot water (170 °C, 60 min) as described by Valoppi et al. [6] and filtered. Before and during the ultrafiltration, the pH was adjusted to neutral (pH 7) to increase and maintain stable the permeate flow through the tubular polyethersulfone membranes (EM006). The concentrate was collected and spray drying (inlet temperature of 170 °C and outlet temperature of 65 °C; drying air flow rate of 667 L/h) [6]. The resulting content was stored in a package protected from light at −20 °C.

2.2. In vitro simulated gastrointestinal digestion

The *in vitro* digestion, which involves specific conditions to simulate *in vivo* oral, gastric, and intestinal phases, was performed following the steps described by Brodkorb et al. [13], with modifications. Briefly, 2 g of GGM were added to falcon tubes, and the oral phase was initiated with salivary fluid (pH 7) and amylase solution (14 U/mg) incubated for 2 min at 37 °C and 150 RPM. Then, gastric fluid (pH 3) and pepsin solution (25,000 U/mL) were added and incubated for 2 h (37 °C and 150 RPM). For the intestinal phase, intestinal fluid (pH 7) was added with pancreatin solution (800 U/mL) and bile salts (160 mM), and the mixture was incubated for 2 h (37 °C and 150 RPM). The reaction was stopped using an ice bath, trichloroacetic acid (2 %, final concentration) was added to eliminate possible interference from the enzymes used during digestion, and the tubes were centrifuged for 10 min at 6000 ×*g*. The supernatant and residues were collected, freeze-dried (LJJ04 JJ Científica®, São Carlos, Brazil), and stored at −20 °C until analysis. All phases of digestion were performed using water as controls, without the addition of digestive enzymes and fluids.

2.3. Chemical profile and antioxidant activity

The total phenolic content (TPC) was determined by the Folin-Ciocalteu reducing capacity as described by Cruz et al. [14], and the results are expressed as mg of gallic acid equivalents per g of GGM (mg GAE/g). (+)-Catechin and (−)-epicatechin were quantified by high-performance liquid chromatography (HPLC) as described by Lima et al. [12], using the Agilent 1100 HPLC device (Agilent Technologies Inc., Espoo, Finland) equipped with diode array detection (DAD) and a Gemini C18 column (150 × 4.6 mm, 5 μm). Separation was performed with a gradient elution of acetonitrile in 5 % formic acid (aq). (+)-Catechin and (−)-epicatechin were quantified at 280 nm. Three replicates were analysed.

Determination of the free monomeric sugars of GGM was performed by gas chromatography (GC), according to Valoppi et al. [6]. Samples were subjected to acid methanolysis, and quantification was performed using six concentration levels for each monosaccharide. Methyl glucuronic acid was quantified based on the D-glucuronic acid standard.

The antioxidant activity of crude and digested extracts was determined by DPPH and FRAP assays using the method described by Granato et al. [3]. All analyses were performed in triplicates, and the results were calculated from an analytical curve, expressed as mg of ascorbic acid equivalent per g of GGM (mg AAE/g).

2.4. Cell culture: viability assay and ROS-generation

To evaluate the cell-based cytotoxicity of the GGM samples (crude and digested), we used the 3-[4,5-dimethylthiazol-2-yl]-2,5-diphenyltetrazolium bromide (MTT) colorimetric assay [15]. For this, SCC-9 (human tongue squamous cell carcinoma), HCT8 (human colorectal ileocecal adenocarcinoma), A549 (human lung epithelial cell adenocarcinoma), and HUVEC (normal human umbilical vein endothelial cell) were used. The cells were seeded into 96-well plates at a density of 1×10^4 and treated with different concentrations of crude and digested GGM (10 to 200 μg GAE/mL). Following the treatment, MTT (0.5 mg/mL) was added to each well and incubated for 4 h. The formazan crystals formed then were dissolved in DMSO and the absorbance was measured at 570 nm. The IC_{50} (50 % cell viability inhibition), GI_{50} (50 % growth inhibition), and LC_{50} (50 % cell death) parameters were performed.

Regarding the intracellular ROS generation, the DCFH-DA assay as a fluorescent probe was employed. The cells were placed in a 96-well plate (6×10^4/well) and, after 24 h to adhesion, were treated with crude and digested GGM (5 to 15 μg GAE/mL) or 22.5 μM H_2O_2 (positive control) and culture medium (negative control). Following the treatment, H_2O_2 (22.5 μM) dissolved in *Hank's* Balanced Salt *Solution (1×)* was added to the wells, and the fluorescence intensity ($\lambda_{emission}$ = 538 nm and $\lambda_{excitation}$ = 485 nm) was measured [15].

2.5. High-throughput synchronous erythrocyte cellular antioxidant activity and protection (HERYCA-P)

The oxidative stress of erythrocytes was induced by 2,2′-azobis(2-amidinopropane) dihydrochloride (AAPH), according to Cruz et al. [14]. First, blood (AB+) was obtained from a female volunteer (30-year-old, healthy, BMI < 25 kg/m^2) and collected in heparinized tubes (University of Limerick – Science and Engineering Research Ethics approval #2023_02_01_S&E). Red blood cells (RBC, haematocrit 20 % in PBS) were mixed with PBS (negative control), ascorbic acid (5 mg/L), or GGM extracts (10 to 100 μg GAE/mL) in polyethylene tubes. After a gentle 20 min of incubation (37 °C, 100 RPM), the mixture was allowed to react with AAPH (200 mmol/L) for 2 h (37 °C, 100 RPM) to complete the oxidation. Then, the mixture was centrifuged at 1200 ×*g* for 10 min, to obtain the supernatant (SN) and the precipitate (PT).

To assess the interaction of GGM and human erythrocytes, 100 μL of SN of each sample or PBS as a blank was transferred to a 96-well microplate and mixed with 200 μL of PBS. Total haemolysis (TH; positive control) was obtained by replacing the sample and AAPH with ultrapure water, and the haemolysis was recorded at 523 nm. The haemoglobin oxidation rate (%) was calculated by the ratio between the 630 nm and 540 nm absorbance, using the same microplate.

Intracellular ROS generation was accessed by washing PT with 400 μL of PBS and centrifuged (1200 ×*g*, 3 min) before adding 400 μL of DCFH-DA solution (10 μmol/L). An aliquot (300 μL) was transferred to a 96-well microplate and incubated in the dark at 37 °C for 20 min. The fluorescence intensity was measured using a microplate fluorometer (Synergy™ H1, Biotek, Waltham, MA, USA) at 485 and 520 nm for excitation and emission, respectively. The results were expressed as a percentage, compared to the negative control (no addition of AAPH).

2.6. *In vivo experimental design*

To conduct the *in vivo* study and following the principles adopted by the Ethics Committee on the Use of Animals (CEUA, nº 0016/2021), male Wistar rats ($n = 36$; 4 weeks old; 94 ± 18 g) were obtained from the Federal University of Alfenas (UNIFAL-MG, Brazil). The rats were maintained at a mean temperature of 23 °C, under 12 h light/dark cycles in individual cages. They were fed *ad libitum* with water and commercial feed (Nuvilab CR-1, Nuvital Nutriente S/A, Colombo, Brazil). The food and water consumption were monitored daily, and the weights of the rats were monitored weekly from the start to the end of the experiment. The treatment with GGM extract was given to all of them by gavage.

Four intraperitoneal injections of 1,2-dimethylhydrazine dihydrochloride (DMH, 40 mg/kg b.w., pH 7) were used to induce animal colon cancer, and ethylenediaminetetraacetic acid solution (EDTA, 1 mM) was used as DMH vehicle in non-induced rats [16]. The injections were administered once a week for four weeks (from the second to the fourth experimental week). The rats were randomly allocated into six groups ($n = 6$ rats per group), divided into G1 (negative control, EDTA), G2 (400 mg/kg of GGM + EDTA), G3 (positive control, DMH), G4 (50 mg/kg GGM + DMH), G5 (200 mg/kg of GGM + DMH), or G6 (400 mg/kg of GGM + DMH).

At the end of the experiment, the feces of each group were collected aseptically before euthanasia. The colon was carefully removed from de rats, and washed with phosphate-buffered saline (PBS, pH 7.4) to remove faecal pellets. The entire colon was opened in a longitudinal incision, fixed for 12 h with 10 % neutral buffered formalin and stored in 70 % ethanol until use for staining [12].

2.7. *Aberrant crypt foci (ACF) and mucin-depleted foci (FDM)*

After fixation, the colon was divided into three fragments: proximal, medial, and distal to the cecum, and stained with 0.2 % methylene blue for 1 min. The frequency of ACF and aberrant crypt (AC) per focus were determined by observing the mucosal side of the colon under conventional microscopy (Nikon Eclipse E100, Minato-ku, Tokyo, Japan) [17]. For further analysis of MDF, the colon segments were stored in 70 % ethanol solution (*v*/v) to remove the methylene blue and placed in a toluidine blue 1 % solution in acetic acid 3 % (v/v) for 5 min. Using the same microscopy (40×), the MDF was identified [12].

2.8. *Effect of GGM on colon histology*

2.8.1. *Histological processing*

Colon fragments were fixed in 10 % buffered formalin (pH 7.2) for 24 h, dehydrated in ethanol, diaphanized in xylene, and embedded in paraffin [16]. Histological sections with 5 μm-thick were obtained in a rotary microtome and stained Alcian Blue and Fast Red for mucin histochemistry detection [18]. Histological sections were obtained in semi-series, collecting one in each of the 20 sections to avoid analysing the same intestinal area. Digital images were obtained using a bright field photomicroscope (Axioscope A1, Carl Zeiss, Germany). Twelve microscopic fields were randomly sampled for each animal using a ×40 objective lens (×400 magnification) [16]. Thus, 62.8×10^5 μm^2 of the colon area was analysed for each group.

2.8.2. *Histopathological and microstructural analysis*

A comparative histopathological analysis of the colon was performed using vehicle-treated rats as a reference for the normal intestinal microstructure. Thus, microscopic evidence of hypertrophy of the lining epithelium, mucosa, and crypts; inflammatory infiltrate, and distribution of goblet cells and lamina propria connective tissue were analysed qualitatively [18,19].

Colon microstructure was quantitatively analysed from 2D computational planimetry using a linear measurement tool ("*drag line feature*") of the image analysis software Image Pro-Plus 4.5® (Media Cybernetics, Rockville, MD, USA) [18]. The number of crypts per histological area was quantified in cross-sections and divided by the image area. The other parameters were estimated from longitudinal sections. Crypts depth and width were quantified from 120 crypts per animal. The width was measured in the middle region of each crypt. Mucosal thickness was calculated as the mean value of the thickness measured in the central area and at two equidistant points at the right and left ends of the histological images [12].

The percentage distribution of mucin was determined utilising a colour-segmentation technique detailed in a prior publication [12]. Briefly, the images underwent conversion to an 8-bit channel and subjected to colour segmentation to black and white. Following the segmentation of mucins in black, Image J was utilized to calculate the histological area occupied by these molecules automatically.

2.9. *Analysis of bacterial content in faecal samples*

To determine the bacterial content, the feces of each group were suspended in sterile saline, and InhibitEX buffer was added before DNA extraction, to avoid any inhibitory effects. The extraction of total DNA was performed using the QIAamp DNA Stool Mini Kit (Qiagen, Inc., Valencia, CA, USA), purified on a QIAamp spin column, and quantified using an Invitrogen Qubit Fluorometer (Thermo Fisher Scientific, Inc., Waltham, MA, USA). The 16S ribosomal RNA genes were analysed in triplicate using specific primers (Table S1) for Bacteroidetes, Firmicutes, and Gammaproteobacteria through the Real-time qPCR technique (StepOne PCR System) [20].

2.10. *Data analysis*

The *in vitro* analyses were performed in quadruplicate and the results were expressed as means followed by the standard deviation. Data with normal distribution were compared using the one-way ANOVA followed by the student-Newman-Keuls and Tukey test. T-test was used to compare crude and digested forms from supernatant or pellet in carbohydrate chemical profile. The histological data are represented as median and interquartile intervals. Data normality was checked using the Shapiro-Wilk test. Nonparametric data were compared using the Kruskal-Wallis One-way ANOVA on the Ranks test. The software used for statistical analysis of all results was GraphPad Prism® software (Version 8.0, USA) and for graphical representations. The data with $p \leq 0.05$ were considered statistically significant.

3. Results and discussion

3.1. *Chemical profile and antioxidant activity of GGM extracts*

The chemical profiles of crude and digested GGM were assessed to understand the effects of the simulated digestion process on bioaccessibility, which represents the proportion of a compound released

from the food matrix during digestion that is accessible for absorption in the small intestine [21]. The crude GGM had a total phenolic content (TPC) of 33 ± 2 mg GAE/g (Table 1), which aligns with the findings of Valoppi et al. [6] (40 mg GAE/g) and Mikkonen et al. [22] (49 mg GAE/g) in an aqueous extract of GGM. Conversely, in the digested GGM extracts (oral, gastric, and intestinal), the TPC value varying from 18 to 21 mg GAE/g. These results suggest that simulation of *in vitro* digestion can decrease the release of phenolic compounds, showing less bioaccessibility.

The bioaccessibility of GGM depends on the composition and structure of the food matrix. For example, dietary fibre can reduce the release of phytochemicals from the food matrix mainly because these compounds have hydrophilic groups that can bind to polysaccharides or cell wall proteins [23]. The classification of GGM as insoluble dietary fibre and its carbohydrate composition ranging between 73 % and 86 % [5] may be the explanation for the low of the compounds.

Enzymatic activity plays an important role in digestion process; therefore, we compared the effects of enzymatic digestion and non-enzymatic digestion on the bioaccessibility of the supernatant compounds in each phase. Interestingly, in the intestinal phase, the bioaccessibility was higher with digestive enzymes (57.5 %) than with the GGM-digested control (53 %), demonstrating an increase of 4.2 %. In contrast, in the oral and gastric phases bioaccessibility was lower (7.2 % and 4.4 %, respectively) in the presence of amylase and pepsin enzymes. Taken as a whole, these results are possibly due to the changes in the pH during digestion. Furthermore, according to Berglund et al. [4], the degradation of GGM increases with increased alkaline hydrolysis, resulting in additional reducing end groups, which can explain the increase in compounds detected in the digested intestinal fraction compared to the gastric and oral phases (Table 1).

The release patterns of catechin and epicatechin was differed from those TPC. Epicatechin exhibited higher values (177 ± 0.3 μg/g) than catechin (45 ± 0.2 μg/g) in undigested GGM, whereas the bioaccessibility in the gastrointestinal tract was 26 % and 15 %, respectively (Table 1). The stability of catechin and epicatechin is considered low under neutral and alkaline pH conditions (owing to their oxidation in these environments). They are considered more stable in acidic environments [24], as demonstrated by our results. Indeed, when the enzyme was removed, it became apparent that the total loss of catechin and epicatechin in the intestinal phase was associated with pH changes.

The concise sketch of the analysis between the pellet (residue) and supernatant relationship revealed a higher phenolic content bioaccessibility in the supernatant (57.5 mg GAE/g) compared to the pellet (50 mg GAE/g) in the intestinal phase, which is the bioavailable part of this matrix. Similarly, the digested GGM supernatant exhibited higher total catechins and epicatechins content than the pellets.

Overall, changes in pH and the presence of digestive enzymes are probable modifying agents of phenolic compounds. Different alterations in physiological conditions (*e.g.*, changes in pH, enzyme activity, bile salts, fluid volumes, and motility) may result in different responses to the digestion of ingested foods or their ingredients, thereby affecting the bioaccessibility of phenolic compounds [21]. Considering these findings, we suggest that the enzymes and pH in the intestine behave as agents that promote the release of phenolic compounds from GGM compared to the mouth and stomach, despite their low general bioaccessibility.

Concerning the carbohydrate composition of GGM, mannose and glucose were the monomers identified in greater quantities in crude and digested GGM, in agreement with the results reported by Berglund et al. [4]. The lack of impact on the bioaccessibility of all monomers in the supernatant following the *in vitro* digestion process (Table 2) could be attributed to the formation of a complex structure known as galactoglucomannan (GGM). This structure is composed of D-mannose (Man) and D-glucose (Glc) units linked together *via* β-(1–4) glycosidic linkages, which are not readily accessible to α-amylases (used in the

Table 1
Content of phenolic compounds, catechins, epicatechins and antioxidant capacity in crude and digested fractions of GGM (supernatants and pellets), as well as their respective controls without the addition of digestive enzymes.

	Samples	TPC (mg GAE/g)	Bioaccessibility (%)	Catechin (μg/g)	Epicatechin (μg/g)	DPPH (mg AAE/g)	Activity (%)	FRAP (mg AAE/g)	Activity (%)
	Crude GGM	33 ± 2^{a}	100 ± 0.00^{a}	45 ± 0.2^{a}	177 ± 0.3^{a}	77 ± 2^{a}	100 ± 0.00^{a}	96 ± 1.5^{a}	100 ± 0.00^{a}
Supernatant	Oral phase								
	Without enzyme	21 ± 0.6^{b}	63 ± 1.8^{b}	42 ± 3^{b}	135 ± 2.5^{bc}	11 ± 0.1^{bc}	14 ± 0.2^{c}	9 ± 0.7^{d}	9 ± 0.7^{e}
	With enzyme	18.5 ± 0.7^{bc}	56 ± 2^{cd}	42 ± 1.5^{b}	140 ± 4.7^{b}	12.5 ± 0.2^{b}	16 ± 0.3^{b}	11 ± 0.5^{bcd}	12 ± 0.5^{cd}
	Gastric phase								
	Without enzyme	20.5 ± 0.7^{b}	70 ± 2.1^{b}	36 ± 0.7^{c}	130 ± 2^{c}	10 ± 0.3^{cd}	13.5 ± 0.4^{d}	13 ± 0.4^{b}	14 ± 0.4^{b}
	With enzyme	19 ± 0.3^{bc}	57.5 ± 1^{c}	36 ± 0.7^{c}	130 ± 3^{c}	11 ± 0.5^{cd}	13 ± 0.6^{d}	10 ± 0.9^{cd}	10 ± 0.7^{de}
	Intestinal phase								
	Without enzyme	18 ± 0.1^{bc}	53 ± 0.3^{de}	33 ± 0.6^{cd}	107 ± 0.8^{d}	8 ± 0.2^{de}	11 ± 0.3^{e}	12 ± 0.4^{bc}	12 ± 0.5^{bc}
	With enzyme	19 ± 0.4^{b}	57.5 ± 1.3^{c}	38 ± 3.5^{bc}	130 ± 2^{c}	10 ± 0.2^{bc}	13 ± 0.2^{d}	10.5 ± 1^{cd}	11 ± 1^{cde}
Pellet	Oral phase								
	Without enzyme	NA	NA	18 ± 2^{e}	52 ± 0.6^{gh}	–	–	–	–
	With enzyme	NA	NA	28 ± 1^{d}	65 ± 0.6^{e}	–	–	–	–
	Gastric phase								
	Without enzyme	NA	NA	8 ± 0.05^{ef}	38 ± 0.8^{i}	–	–	–	–
	With enzyme	NA	NA	13 ± 0.3^{ef}	57 ± 0.4^{fg}	–	–	–	–
	Intestinal phase								
	Without enzyme	18 ± 0.4^{c}	55 ± 1.2^{cd}	10 ± 0.6^{ef}	61 ± 0.7^{ef}	8 ± 0.07^{de}	11 ± 0.1^{e}	11 ± 0.4^{bc}	12 ± 0.4^{cd}
	With enzyme	17 ± 0.2^{c}	50 ± 0.6^{e}	7 ± 0.3^{f}	49 ± 0.2^{h}	7 ± 0.04^{e}	10 ± 0.05^{f}	10 ± 0.9^{cd}	10.5 ± 0.9^{cde}

Note: GGM, galactoglucomannan; TPC, total phenolic content; DPPH, 2,2-diphenyl-1-picrylhydrazyl; FRAP, Ferric Reducing Antioxidant Power; GAE, gallic acid equivalent; AAE, ascorbic acid equivalent. Means ± SD. Different letters in the same column reveal statistical differences using the Tukey test ($p < 0.05$).

Table 2
Carbohydrate composition (expressed as mg/g of sample ± standard error) for GGM supernatant and pellet in crude sample and solution resulting from *in vitro* digestion process (intestinal phase).

Carbohydrate (mg/g)	Supernatant		Pellet	
	Crude GGM	Digested GGM intestinal phase	Crude GGM	Digested GGM intestinal phase
Mannose	360 ± 14[a]	337 ± 49[a]	59 ± 1[b]	31 ± 0.8[c]
Glucose	92 ± 4[a]	92.8 ± 14[a]	15 ± 0.4[b]	9 ± 0.3[c]
Galactose	48 ± 2[a]	48.5 ± 7[a]	8 ± 0.1[b]	4 ± 0.2[c]
Xylose	54 ± 2[a]	50.4 ± 7[a]	9.5 ± 0.2[b]	5 ± 0.1[c]
Arabinose	2 ± 0.4[a]	2 ± 0.6[a]	0.4 ± 0.01[b]	0.2 ± 0.03[b]
Rhamnose	3 ± 0.2[a]	3 ± 0.5[a]	0.6 ± 0.00[b]	0.3 ± 0.01[c]
Glucuronic acid	n.d.	n.d.	n.d.	n.d.
Galacturonic acid	11 ± 4[a]	12 ± 1.7[a]	2 ± 0.2[b]	1 ± 0.02[b]
Methylglucuronic acid	5 ± 0.3[a]	4 ± 0.6[a]	0.7 ± 0.07[b]	0.4 ± 0.01[c]

Note: n.d. = not detected; GGM, galactoglucomannan. Different letters in the same line are significantly different comparing crude and digested forms from supernatant or pellet (*t*-test $p < 0.05$).

INFOGEST protocol) responsible for breaking down polysaccharides. Hence, the resistance of GGM to digestion may explain the unchanged bioaccessibility of the monomers during *in vitro* digestion. Additionally, the reduction in monomers observed in the pellet during digestion was insufficient to induce discernible difference in the bioaccessibility of the supernatant.

The impairment of gastrointestinal digestion in GGM resulted in an antioxidant activity (DPPH and FRAP) corresponding to 9–16 % of that in undigested GGM (Table 1), showing a decrease in antioxidant capacity after the *in vitro* digestion process. Thus, the decreased antioxidant activity after digestion might not be sufficient to be physiologically relevant. The presence of digestive enzymes was responsible for the antioxidant changes induced by digestion process. Compared to the fractions without enzymes, the digestive enzymes decreased FRAP in the gastric and intestinal phases (from 13 to 10 mg AAE/g and from 12 to 10.5 AAE/g, respectively) and increased DPPH in the intestinal phase (from 8 to 10 mg AAE/g).

Phenolic compounds, particularly epicatechin, are directly related to antioxidant capacity owing to their capacity for single electron-proton transfer (DPPH) and reduction of iron (FRAP); they mainly possess four hydroxyl groups, two of which are in *ortho* position (B ring) and two hydroxyl groups in meta position (A ring), involving oxidation at both rings [25]. The chemical structure is susceptible to hydrolysis, which occurs during digestion, reducing deprotonation and leading to instability and a decreased ability to scavenge free radicals [21]. Although sugar monomers may not be as potent antioxidant as certain polyphenols, they still contribute to the overall antioxidant capacity, since the hydrolysis results in additional reducing end groups (OH) that can donate hydrogen atoms to ROS, or chelating transition metals ions, influencing oxidative stress levels [4]. These events are aligned with the results obtained in our current study, where no significant difference was observed between the content of the crude and digested supernatants in terms of monomers, which indicates that the decrease in the bioaccessibility of phenolic compounds after digestion in action of the gastrointestinal tract leads to lower antioxidant capacity.

Although these effects were observed in the chemical analysis, different behaviours were found in the antioxidant evaluation in cell culture, as presented in the *in vitro* cellular and animal experiments where GGM an anticarcinogenic effect.

3.2. Cytotoxicity assessment

Cytotoxicity was assessed using normal and cancer cell lines, showing that the mechanisms of action of undigested and digested GGM were not the same (Table 3). SCC-9, HCT-8, and HUVEC cell growth was inhibited by undigested and digested GGM as they exhibited low viability (IC_{50}) and lethal values (LC_{50}). On the other hand, A549 cells were the most resistant to the action of the extracts (IC_{50} ranged from 100 to >200 μg GAE/mL) and did not reach lethal values ($LC_{50} > 200$ μg GAE/mL). A similar result was found by Ferreira-Santos et al. [26], who demonstrated that the cell viability of the same cell line was not verified up to the maximum mass concentration ($IC_{50} > 1000$ μg/mL) of *Pinus pinaster* bark aqueous extracts. Moreover, Granato et al. [3] identified high IC_{50}, GI_{50}, and LC_{50}, values (>1000 μg/mL) for the GGM extract in A549, HCT-8, HepG2, and IMR90 cell lines.

We considered the cytotoxicity classification mentioned by Anywar et al. [27], where GGM is classified as highly active if $IC_{50} \leq 20$ μg/mL, moderately active if $IC_{50} = 21$–200 μg/mL, weakly active if $IC_{50} = 201$–500 μg/mL and inactive if $IC_{50} \geq 501$ μg/mL. Based on this classification, the digested samples exhibited high to moderate cytotoxicity against the cell lines tested, with SCC-9 and HUVEC cell lines being the most sensitive to crude and digested GGM extracts with low estimated values of IC_{50} (19 to 168 μg GAE/mL), growth inhibition ($GI_{50} = 2$ to 114 μg GAE/mL), and lethal values (LC_{50} ranged from 25 to 178 μg GAE/mL). Comparison of the crude and digested forms, revealed that *in vitro* digestion reduced the toxicity of GGM, increasing the values of IC_{50}, GI_{50}, and LC_{50} by up to five times. Indeed, when we performed blood cell assays (Section 3.4) and *in vivo* experiments (Sections 3.6–3.8), no toxicological effects were observed; instead, protective effects were highlighted. Therefore, additional studies are warranted to explore the potential cellular mechanisms involved and to assess the safety of GGM for use as a food ingredient.

3.3. Intracellular ROS-generation

In this study, GGM showed, in general, a protective antioxidant effect on the three cancer cell lines evaluated, without inducing the formation of ROS, and protecting in the presence of H_2O_2, mainly in the digested fraction (Fig. 1A-I). A different behaviour was observed in the normal cell line (HUVEC), in which both the oral and intestinal phases of undigested GGM simultaneously increased the level of ROS in the presence of H_2O_2, thereby increasing the oxidation levels above those of the positive control (Fig. 1J-L). Interestingly, oral and intestinal enzymes significantly changed this profile, contributing to the antioxidant effect of these two phases with or without H_2O_2, reaching levels below the cellular baseline as the dose increased. By our results, Granato et al. [3] found a pro-oxidant effect of crude GGM extract in A549 and HCT-8 cancer cell lines, and in a non-cancerous cell line (IMR90), the GGM extract was able to restore ROS levels to the same magnitude as spontaneous generation.

Phenolic compounds have dual-faced properties, acting as both pro-oxidant and antioxidant agents, depending on several factors, such as their concentration, structure, and environment [25]. *In vitro* digestion causes interference with the biological effects in enzymatic, mechanical, and biochemical extractions of macronutrients and micronutrients [9]. In addition, the number of hydroxyl groups, solubility, and nature of the substituents on the aromatic rings play crucial roles in their bioactivity [28]. Our results indicated that the GGM is a complex matrix that plays a vital role in protecting cells from the potentially harmful effects of the ROS generation. Gastrointestinal digestion affects the protective potential of GGM, mostly in normal cells. Thus, the amount of phenolic compounds does not explain this cellular effect, as the reduced antioxidant chemical profile in undigested GGM extracts did not correspond to the cellular antioxidant activity found.

Table 3
Cytotoxicity, cell growth inhibition and lethal parameter of SCC-9, A549, HCT8, and HUVEC cells after 48 h exposure to undigested and digested GGM expressed in μg GAE/mL of GGM extracts.

Cell Lines	GGM extracts					
	Undigested oral phase (μg GAE/mL)	Digested oral phase (μg GAE/mL)	Undigested gastric phase (μg GAE/mL)	Digested gastric phase (μg GAE/mL)	Undigested intestinal phase (μg GAE/mL)	Digested intestinal phase (μg/GAE/mL)
SCC9	$IC_{50} = 30$	$IC_{50} = 54$	$IC_{50} = 21$	$IC_{50} = 45$	$IC_{50} = 23$	$IC_{50} = 123$
	$GI_{50} = 10$	$GI_{50} = 9.5$	$GI_{50} = 9.5$	$GI_{50} = 2$	$GI_{50} = 16$	$GI_{50} = 24$
	$LC_{50} = 39$	$LC_{50} = 59$	$LC_{50} = 27$	$LC_{50} = 59$	$LC_{50} = 25$	$LC_{50} = 148$
A549	$IC_{50} = 148$	$IC_{50} > 200$	$IC_{50} = 108$	$IC_{50} = 192$	$IC_{50} = 100$	$IC_{50} > 200$
	$GI_{50} = 118$	$GI_{50} = 118.$	$GI_{50} = 95$	$GI_{50} = 155$	$GI_{50} = 71$	$GI_{50} = 126$
	$LC_{50} > 200$	$LC_{50} > 200$	$LC_{50} > 200$	$LC_{50} > 200$	$LC_{50} > 200$	$LC_{50} > 200$
HCT8	$IC_{50} = 34$	$IC_{50} = 77$	$IC_{50} = 37$	$IC_{50} = 70$	$IC_{50} = 42$	$IC_{50} = 166$
	$GI_{50} = 25$	$GI_{50} = 34$	$GI_{50} = 26.5$	$GI_{50} = 24$	$GI_{50} = 27$	$GI_{50} = 37$
	$LC_{50} = 49$	$LC_{50} = 99$	$LC_{50} = 49.5$	$LC_{50} = 123$	$LC_{50} = 83$	$LC_{50} = 200$
HUVEC	$IC_{50} = 19$	$IC_{50} = 83.5$	$IC_{50} = 21$	$IC_{50} = 94$	$IC_{50} = 35$	$IC_{50} = 168$
	$GI_{50} = 15$	$GI_{50} = 55.5$	$GI_{50} = 22.5$	$GI_{50} = 72$	$GI_{50} = 25$	$GI_{50} = 114$
	$LC_{50} = 34$	$LC_{50} = 94$	$LC_{50} = 49$	$LC_{50} = 107$	$LC_{50} = 50$	$LC_{50} = 178$

Note: SCC-9 (human tongue squamous cell carcinoma); A549 (human lung epithelial cell adenocarcinoma); HCT8 (human colorectal ileocecal adenocarcinoma); HUVEC (normal human umbilical vein endothelial cell); GAE, gallic acid equivalent. IC_{50} (concentration of extracts that inhibit cell viability by 50 %); GI_{50} (concentration of extracts that inhibits cell growth by 50 %); and LC_{50} (concentration of extracts that result in 50 % loss of cells).

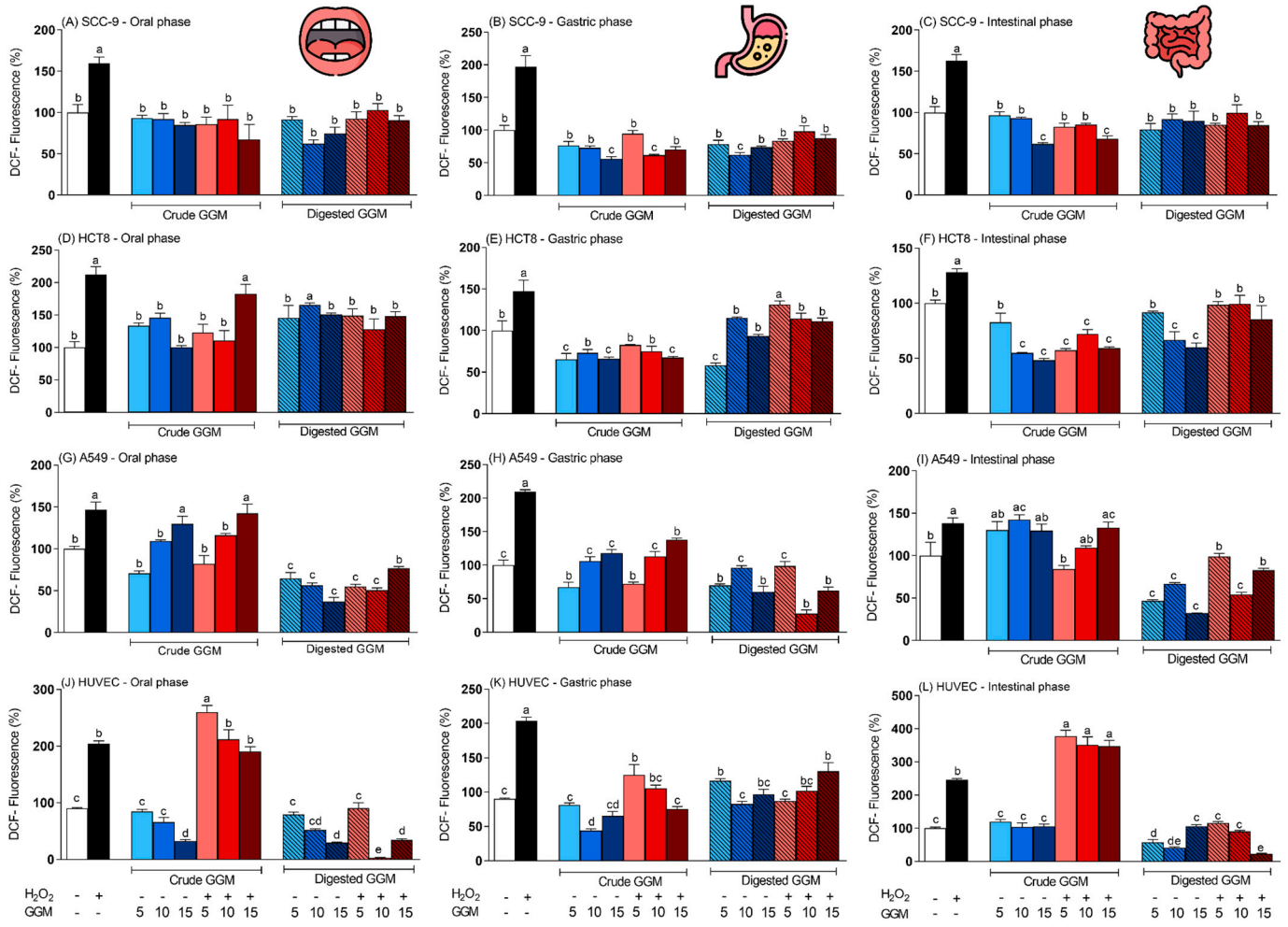

Fig. 1. Results of intracellular ROS measurement by DCF-fluorescence using spectrofluorimetric analysis. Treatment with crude and digested fractions of GGM (oral, gastric, and intestinal) at 5–15 μg GAE/mL, and H_2O_2 (22.5 μM) were tested in SSC-9 (A, B, and C), HCT8 (D, E, and F), A549 (G, H, and I), and HUVEC (J, K, and L) cells. Quantitative data are the mean ± SD. Different letters represent statistical differences ($p < 0.05$).

3.4. GGM protection of human erythrocytes against AAPH-induced stress

Using the HERYCA-P protocol, we used AAPH as the oxidative agent and human red blood cells (RBC) as the test model. Herein, we observed that AAPH-treated RBC pre-incubated with GGM extracts (crude and digested) showed lower dichlorofluorescein (DCF) fluorescence intensity (Fig. 2A). This result indicates that GGM extracts reduced AAPH-induced oxidative stress, by acting as antioxidant agent, mainly derived

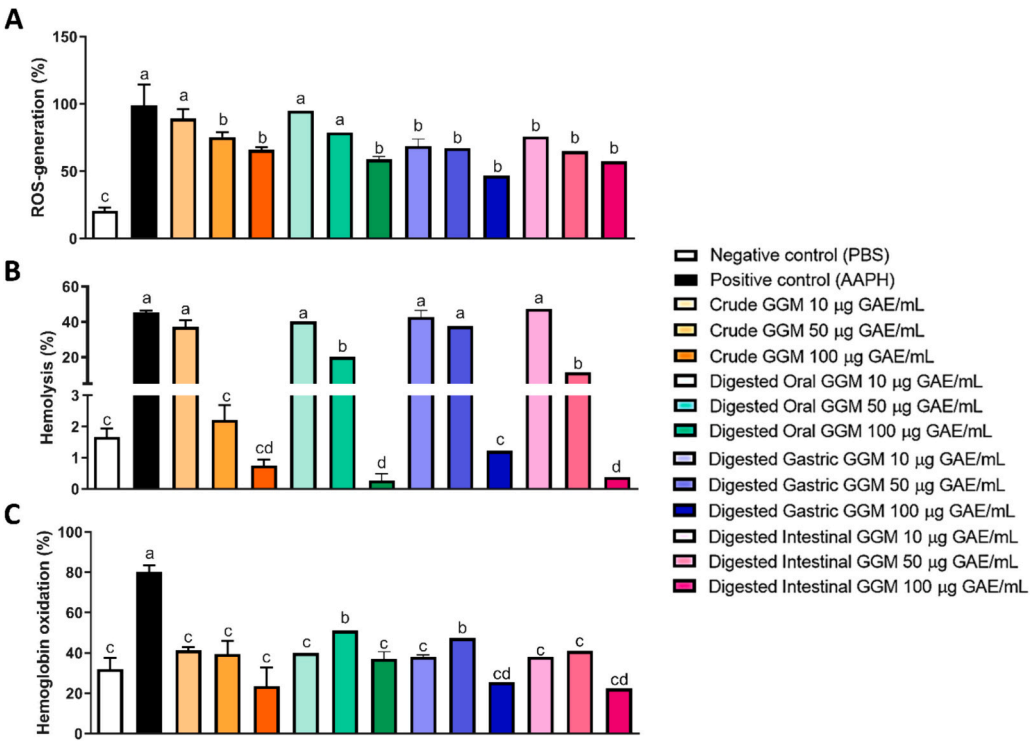

Fig. 2. Effect of GGM on intracellular reactive oxygen species (ROS) generation (A), hemolysis (B), and haemoglobin oxidation (C) in human erythrocytes, induced by 2′-azobis(2-amidinopropane) dihydrochloride (AAPH). Different letters reveal statistical differences ($p < 0.05$).

from the antioxidant potential of phenolic compounds present in the samples. It is well-known that phenolic-rich foods and extracts can mitigate oxidative stress and reduce the rate of haemolysis [14].

One of the consequences of AAPH-induced oxidative stress in RBC is haemolysis and haemoglobin oxidation, which occur because of the oxidation of membrane lipids and proteins, affecting the balance and resilience of the erythrocyte membrane and swelling of RBC [14]. GGM extracts suppressed haemolysis *in vitro* in the RBC by reducing the AAPH-induced haemolysis rate in a concentration-dependent manner ($p < 0.05$) from 45 % (positive control) to 0.4 % (100 µg GAE/mL, intestinal phase) (Fig. 2B). They protected against haemoglobin oxidation reached at basal RBC levels (Fig. 2C). This protection occurs at any stage of *in vitro* digestion and in the same way as that of crude GGM, showing erythrocyte membrane-protective activity even if the bioaccessibility of compounds appears lower after digestion.

The antihaemolytic effect of human erythrocytes is not only associated with phenolic compounds, but also with carbohydrates impact this property when they interact with phenolics and form a colloidal system that acts as a physicochemical barrier that impedes haemolysis [3]. Although GGM decreased oxidative stress in human RBC, these results do not mirror those behaviour of previous chemical antioxidant assays.

3.5. Effect of GGM on in vivo nutritional and metabolic parameters

To confirm the health and well-being of the rats during the experiment, we evaluated body mass gain, food and water consumption, caloric intake, feed efficiency, and metabolic parameters (Table S2). Careful observation during the experimental period (6 weeks) revealed that no treatment-related deaths occurred in any of the groups. Regarding the weight of the animals, although all rats exhibited body mass gain during the experiment (5 ± 0.4 g/rat, day), the groups that received EDTA and EDTA +400 mg/kg GGM extract exhibited higher mass gain compared to that in the groups that received DMH. This result provides evidence that the inflammatory process generated by the complex metabolic activation of DMH decreases body mass gain [29]. Interestingly, the DMH administration did not interfere with metabolic parameters (MGR and SGR), feed efficiency (FER and PER), hunger, or water consumption. Moreover, although GGM is a fibre, it did not increase water consumption by rats. Together, these results demonstrate that the three doses of GGM administered by gavage and the induction of cancer with DMH did not cause nutritional changes that were detrimental to the well-being of the experimental rats.

3.6. Effect of GGM on ACF e MDF induced by DMH

In the present study, the groups that received only the EDTA vehicle (negative control) and EDTA+400 mg/kg GGM (GGM control) did not show changes compatible with colon carcinogenesis. They did not induce the presence of ACF (Fig. 3A). This result provides vital safety parameters for the administration of GGM at the highest dose (400 mg/kg), suggesting evidence that it does not serve as a pro carcinogenic factor associated with the development of classic aberrant crypt foci at this dosage.

As expected, based on the literature, the groups that received DMH presented ACF (Fig. 3B), described as a group of lesions used as a suitable biomarker to evaluate predisposition to colon carcinogenesis in animal models [17]. The association between DMH and the maximum dose of GGM administered (400 mg/kg) had a protective effect against the predisposing of colorectal cancer, with a reduction in hyperplasia throughout the colon, as observed by the decrease in the number of ACF by 34.9 % (Fig. 3C). This aspect reinforces the carcinogenic capacity of DMH by stimulating the classic formation of aberrant crypts and the ability of GGM to reduce the preneoplastic effect in the distal colon, of the most common location of CRC [29].

The multiplicity of crypts (number of crypts per focus) is also essential for evaluating the growth of ACFs and is more predictive of malignant transformation than the number of ACFs [12]. There is a hypothesis that many ACFs regress and only larger foci of aberrant crypts progress to cancer [16]. A more significant number of crypts ≤ 2/focus was observed, compared to the number of crypts ≥ 3/focus, in all

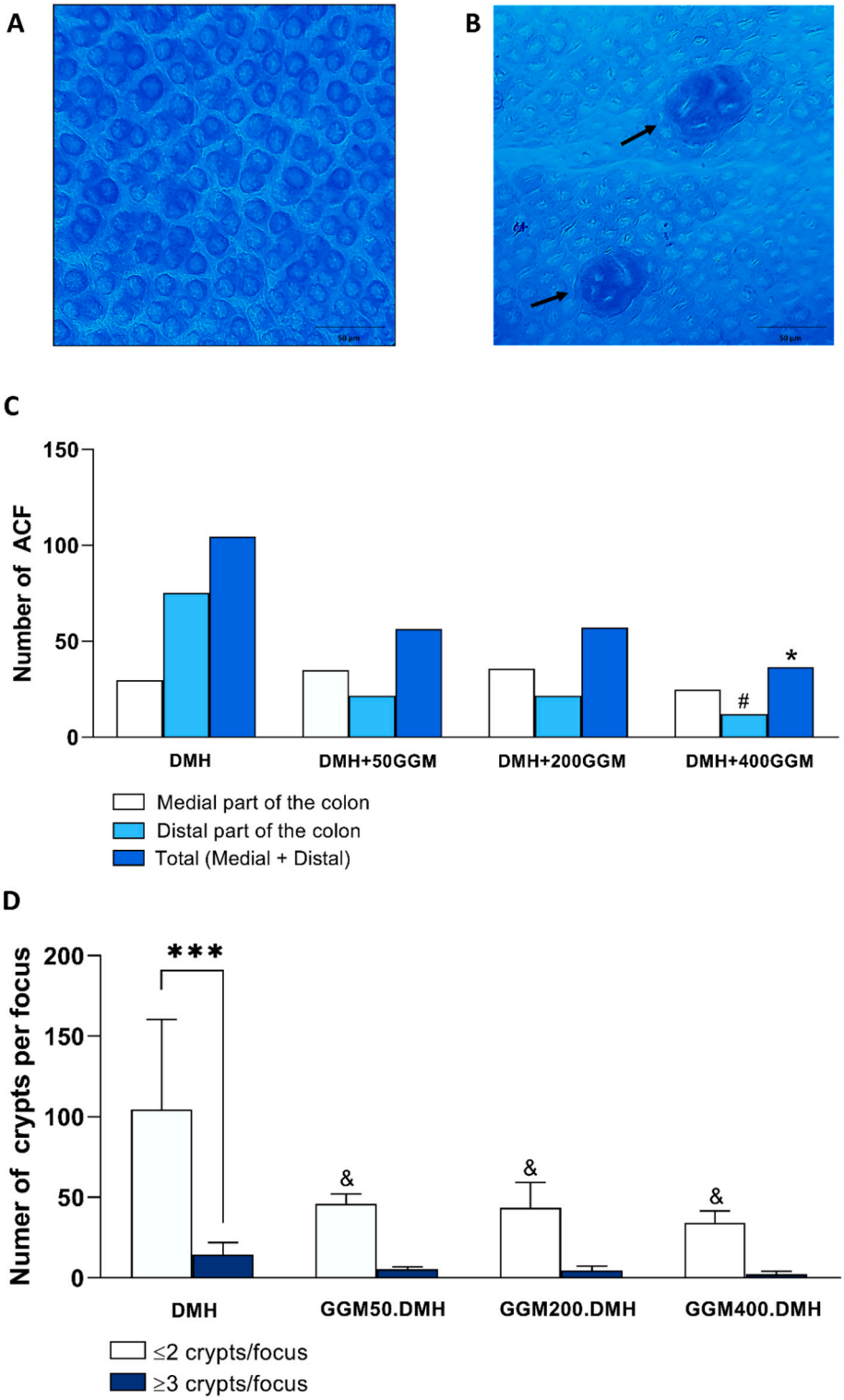

Fig. 3. (A) Microscopic topographic view of an area with unchanged colony crypts; (B) Two classic ACF-methylene blue stains, with four aberrant crypts each (arrow); (C) number of ACF present in the medial, distal segment and the total number of ACF in the entire colon; (D) number of crypts present per focus. DMH = 1,2-dimethylhydrazine (4 × 40 mg/kg b.w.), GGM = galactoglucomannan extract; 50, 200 and 400 indicate the amount of gavage (mg/kg b.w.). Different superscript signs in each column indicate significant differences ($p < 0.05$), with # related to distal DMH, * related to total DMH, *** related to DMH ≥ 3 crypts and & related to DMH ≤ 2 crypts.

groups evaluated in this study, which can be explained by the short duration of the experiment after carcinogenesis induced with DMH (Fig. 3D). Our results showed that GGM attenuated the initiation and progression of neoplastic lesions by reducing the multiplicity of crypts, even at the minimum dose administered (50 mg/kg). Lee et al. [30] found similar results using cereals rich in insoluble dietary fibre and phenolics (Chenopodium formosanum [djulis]), which showed strong inhibitory effects and produced a significant reduction in the number of small aberrant crypts. These findings can be explained by the action of phenolic and carbohydrate compounds in GGM, which provide evidence

of their biological activities even at lower concentrations.

Notwithstanding, GGM is a potentially effective matrix for preventing colon carcinogenesis during the early stages of ACF development. This is mainly due to the levels of phenolic compounds that demonstrate a potential antiproliferative effects on human cancer cells through inhibitory and lethal actions on cell growth *in vitro*, in addition to apoptotic action and regulation of the main pathways involved in the aetiology of this neoplasm [31]. Few studies have investigated the potential of phenolic compounds from tree bark on the initiation and progression of colon cancer in animal models. To our best of knowledge, this is the first study to describe the effects of a galactoglucomannan-rich extract of Norway spruce sawdust on colorectal carcinogenesis.

3.7. Effect of GGM on the histological and microstructural parameters in the colon

As shown in Fig. 4A, the histopathological analysis of longitudinal sections revealed well-defined intestinal crypts surrounded by the lamina propria with moderate cellularity in the intestinal mucosa of all groups. A slight thickening of the intestinal mucosa was observed in all groups exposed to DMH. Epithelial thickening, characterised primarily by enterocytes with an elongated nuclear profile, was observed in the DMH and DMH + 50 mg/kg GGM groups. In addition, increased crypt depth was identified in the DMH + 200 mg/kg GGM group. Mucin depletion was observed in the DMH and DMH + 50 mg/kg GGM groups. However, no morphological evidence of inflammatory infiltration was detected in any of the groups.

Microscopic observation of the cross sections (Fig. 4B) revealed many crypts with narrow lumens and small profiles interspersed by narrow connective tissue areas in the EDTA and EDTA+400 mg/kg GGM groups. The cross-sectional profile of intestinal crypts shows variable hypertrophy in all groups exposed to DMH. In addition to hypertrophy, a low distribution of crypts with a dilated lumen and connective tissue expansion was observed in the DMH and DMH + 50 mg/kg GGM groups.

As shown in Fig. 4C, quantitative microstructural analysis reinforced the histopathological findings, indicating a marked increase in the lining epithelium height, crypt depth, and crypt width in the DMH and DMH + 50 mg/kg GGM groups compared to the control groups (not exposed to DMH). Crypt number and mucin distribution were reduced in all DMH-exposed groups compared to those DMH-untreated rats. Mucosal thickness and crypt depth were higher in all DMH-exposed groups, except that in the DMH + 400 mg/kg GGM group, than in DMH-untreated rats. Mucin depletion was attenuated, the number of crypts was higher, and epithelial height was reduced in the DMH + 200 mg/kg GGM and DMH + 400 mg/kg GGM groups compared to that in the DMH group.

3.8. Effect of GGM on gut bacterial composition

To better understand the relationship between the consumption of GGM and the modulation of gut bacteria, the effects of GGM and DMH on rat microbiota were investigated (Fig. 5). Bacterial microbiota is known to influence the absorption and metabolism of dietary polyphenols in the small intestine. Polyphenols can act as prebiotics that modulate the growth of specific bacterial strains and contribute to the maintenance of health status [10]. Our results showed that the DMH and GGM groups (EDTA+400 mg/kg GGM) had a decreased abundance of total bacteria compared to healthy rats (EDTA group). Interestingly, DMH and the highest dose of GGM, increased bacterial abundance, equalling that of healthy rats. These variations can be explained by dynamic changes in the intestinal microbiome due to a combination of genetic, epigenetic, and local factors [32], including interactions between Bacteroides (which have β-glucuronidase activity) and azoxymethane (an active compound carcinogen) [33]. Moreover, GGM, a fermentable carbohydrate used by probiotic bacteria, is readily absorbed in the large intestine [8].

The composition of anaerobic bacteria in a healthy intestinal environment is important, because they comprise Firmicutes and Bacteroidetes. The ratio of these two bacteria phyla (F/B) indicate a balance in normal intestinal microbiota [12]. In this study, we found that DMH decreased the abundance of both species compared to that in healthy rats, and GGM (400 mg/kg) modulated the intestinal microbiota by maintaining Bacteroidetes and reducing the abundance of Firmicutes, deregulating the relationship between them, and promoting dysbiosis. The analysis of the F/B ratio confirms these findings, showing that GGM reduced it to negative values (-56 ± 19) (Table S3). A decrease in the F/B ratio characterises inflammatory bowel disease and signifies a decrease in Firmicutes and an abundance of Bacteroidetes [34]. However, the histopathological findings of this study confirmed the absence of inflammatory infiltrates in all the groups investigated. On the other hand, GGM seems potentially beneficial for the intestinal microbiota only at its lowest dosage (50 mg/kg) ($F/B = 79 \pm 28$).

Interestingly, the interaction between GGM and DMH increased the F/B ratio by up to 318.61 % compared to that in healthy rats. The increase in the F/B ratio is generally associated with obesity in experimental animals [34], which was not observed in the nutritional parameters of the rats in this study, keeping these findings still incipient. The maintenance of Bacteroidetes abundance by GGM can be explained by the fact that the genomes of these bacteria encode a large number of carbohydrate-inducible active enzymes that allow for the use of dietary and host mucosal glycans [33]. A recent study indicated that galactoglucomannan may positively modify the composition of the intestinal microbiota and increase the production of short-chain fatty acids in feces, exerting desirable effects on both inflammatory bowel disease and colorectal cancer [11].

Furthermore, none of the treatments used in this study modulated Gammaproteobacteria, which are considered potentially pathogenic; their increase would be expected at least in the DMH group, as they have the most significant inflammatory potential [16]. For example, *E. coli* is a pathogenic bacterium belonging to the Gammaproteobacteria class with a deficient capacity to ferment softwood hemicelluloses such as GGM [2]. Therefore, the dysbiotic intestinal microbiome resulting from treatment with GGM, which is potentially less harmful at its lowest dose, is not compatible with the histopathological findings and the presence of pre-neoplastic changes in the colons of rats treated with low doses of GGM.

4. Conclusions

GGM proved to be an excellent source of phenolic compounds with high antioxidant capacity. However, the gastrointestinal tract reduces this antioxidant capacity, making these compounds less bioaccessible by the end of digestion process. Despite that, GGM exhibited a strong cytotoxic and antiproliferative effects and reduced the damage caused by oxidative stress in human cells, possibly owing to the action of the phenolic compounds present in the extracts. Regarding the *in vivo* experiment, GGM at the highest dose attenuated the appearance of pre-neoplastic lesions and morphological changes in the colonic tissue. Even though GGM is known as a fermentable fibre that promotes intestinal health, when associated with DMH, may induced dysbiosis, keeping this correlation still incipient, with the prospect of being potentially safe for the intestinal bacterial microbiome at lower doses, encouraging future investigations. Considering the relative toxicological safety of GGM demonstrated using different biological assays, resources from the forestry industry, which have been considered a by-product with limited use until now, represent a potential resource for the production of new functional ingredients for food and pharmaceutical applications.

Supplementary data to this article can be found online at https://doi.org/10.1016/j.ijbiomac.2024.133986.

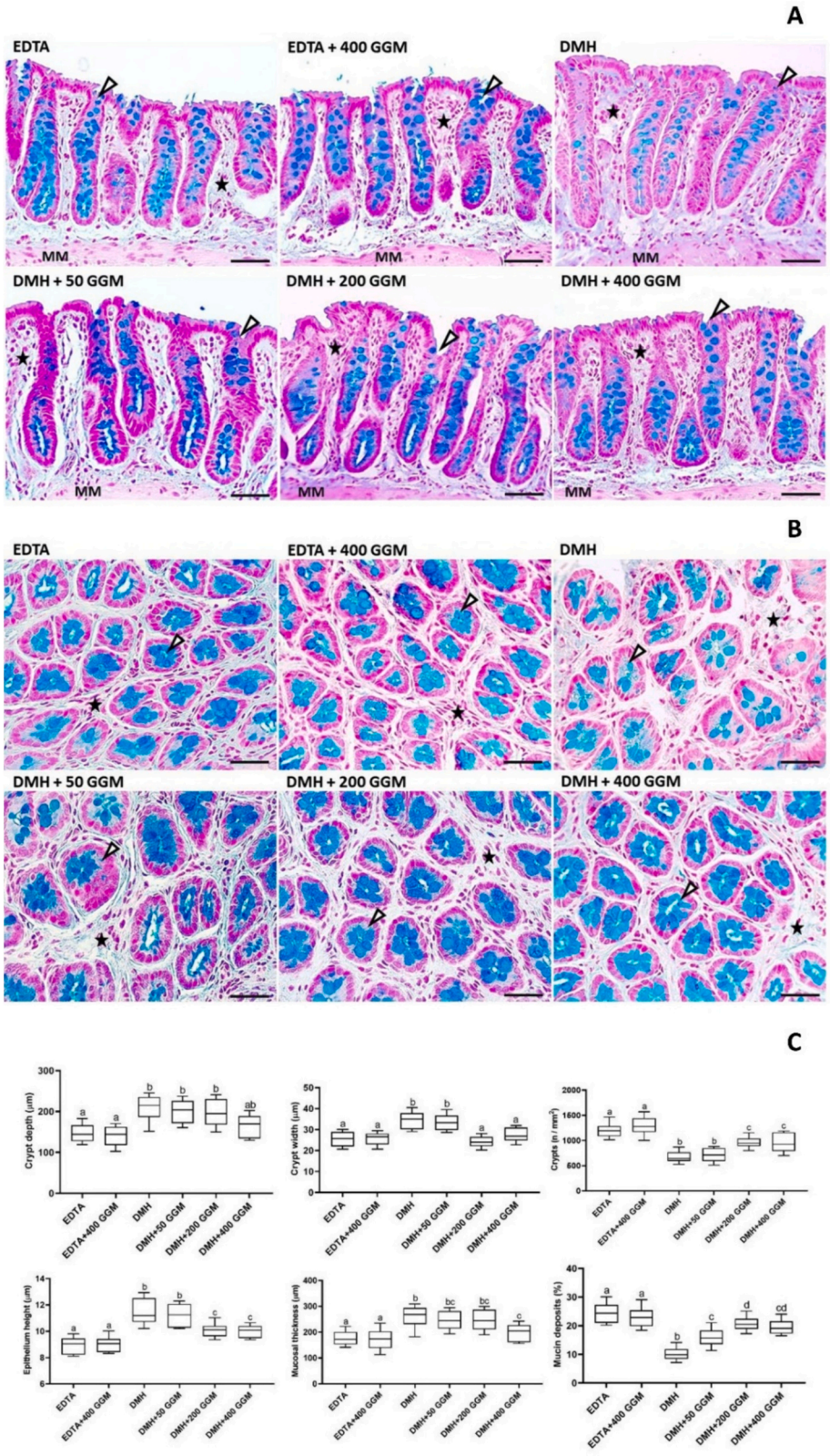

Fig. 4. (A) Microscopic images of the colon of rats treated with dimethylhydrazine (DMH) and different concentrations of galactoglucomannan (GGM) (Longitudinal sections, brightfield microscopy, Alcian Blue staining, scale bar = 40 μm). (B) Microscopic images indicating the distribution of mucins and intestinal crypts of rats treated with DMH and different concentrations of GGM (Cross-sections, brightfield microscopy, Alcian Blue staining, scale bar = 40 μm). (C) Colon microstructure in rats treated with DMH and different concentrations of GGM. Arrowheads: Intestinal crypts. Star: lamina propria (loose connective tissue). Cell nuclei are stained in red and mucins in blue. Results are expressed as median and interquartile interval. Different letters in the columns indicate statistical difference among the groups ($p < 0.05$). Groups treated with: EDTA = EDTA, EDTA + 400 GGM = EDTA and 400 mg/kg GGM, DMH = DMH, EDTA + 50 GGM = EDTA and 50 mg/kg GGM, EDTA + 200 GGM = EDTA and 200 mg/kg GGM, EDTA + 400 GGM = EDTA and 400 mg/kg GGM.

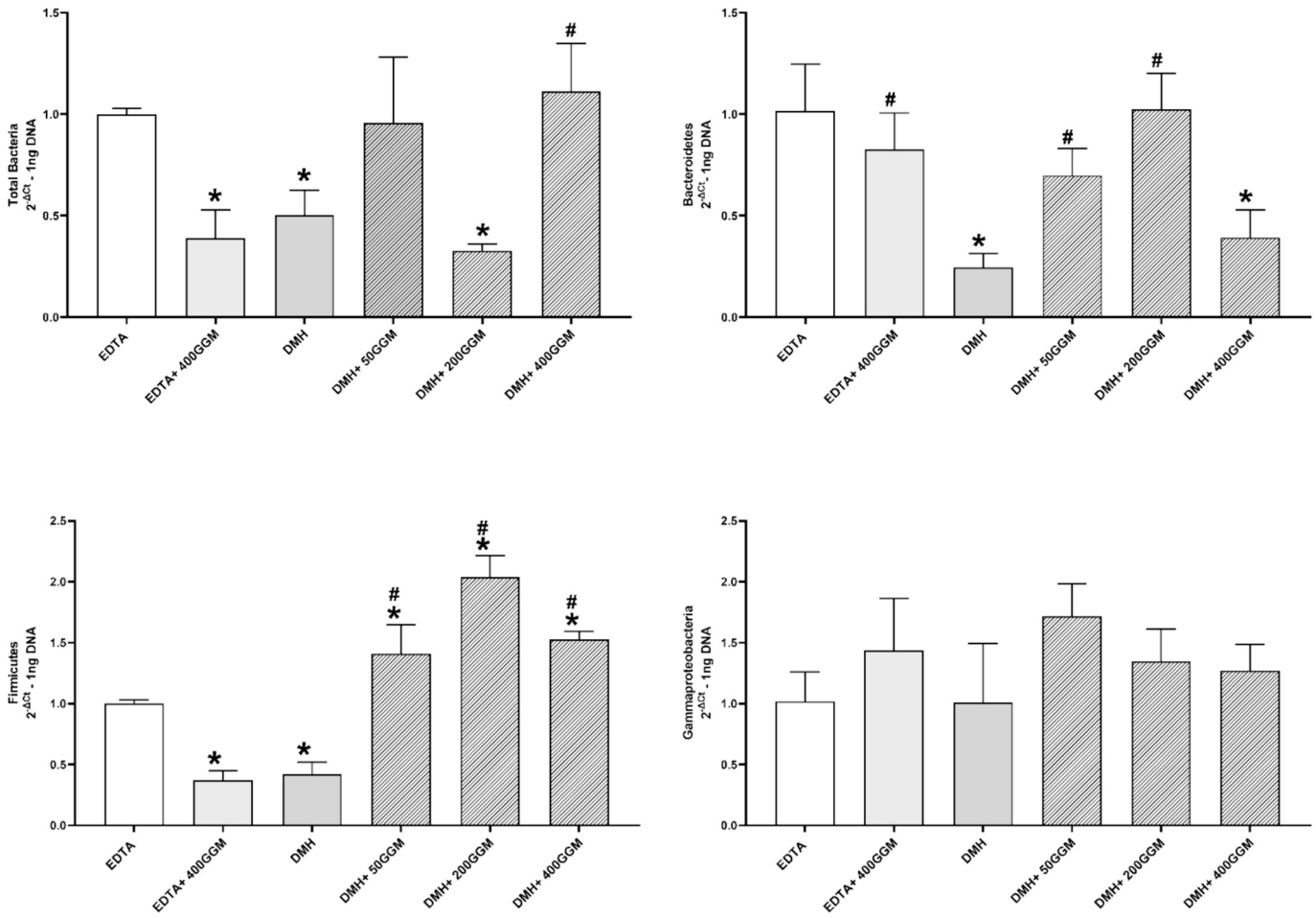

Fig. 5. Effect of GGM on modulating the intestinal microbiota. EDTA, ethylenediaminetetraacetic acid; GGM, galactoglucomannan; DMH, 1,2-dimethylhydrazine. 50, 200 and 400 is related to mg/kg of GGM extract. Different superscript signs in each column indicate significant differences ($p < 0.05$), with * related to EDTA control (negative control), # related to DMH (positive control).

CRediT authorship contribution statement

Amanda dos Santos Lima: Writing – original draft, Methodology, Formal analysis. **Fernanda Rafaelly de Oliveira Pedreira:** Writing – original draft, Methodology, Formal analysis. **Nathália Alves Bento:** Formal analysis. **Rômulo Dias Novaes:** Writing – original draft, Formal analysis. **Elda Gonçalves dos Santos:** Writing – original draft, Formal analysis. **Graziela Domingues de Almeida Lima:** Writing – original draft, Formal analysis. **Leonardo Augusto de Almeida:** Formal analysis. **Thiago Caetano Andrade Belo:** Formal analysis. **Fernando Vitor Vieira:** Formal analysis. **Nima Mohammadi:** Formal analysis. **Petri Kilpeläinen:** Writing – original draft, Supervision, Methodology, Funding acquisition, Data curation, Conceptualization. **Alexandre Giusti-Paiva:** Formal analysis. **Daniel Granato:** Writing – original draft, Supervision, Methodology, Funding acquisition, Data curation, Conceptualization. **Luciana Azevedo:** Writing – original draft, Supervision, Methodology, Funding acquisition, Data curation, Conceptualization.

Declaration of competing interest

The authors declare the following financial interests/personal relationships which may be considered as potential competing interests: Luciana Azevedo reports financial support was provided by Minas Gerais State Foundation of Support to the Research. Luciana Azevedo reports financial support was provided by National Council for Scientific and Technological Development.

Data availability

Data will be made available on request.

Acknowledgments

We are grateful for the financial support provided by Minas Gerais State Research Support Foundation (FAPEMIG) [grant number: APQ-04299-22; APQ-02221-24] and National Council for Scientific and Technological Development (CNPq) [grant number: 422096-2021-0; 306799/2021-9; 402546/2022-9]. Flaticon is also acknowledged for the icons used in the graphical abstract and figures.

References

[1] S. Spinelli, C. Costa, A. Conte, N.L. Porta, L. Padalino, M.A.D. Nobile, Bioactive compounds from Norway spruce bark: comparison among sustainable extraction techniques for potential food applications, Foods 8 (2019) 110524, https://doi.org/10.3390/foods8110524.

[2] V. Deloule, C. Boisset, D. Hannani, A. Suau, A. Le Gouellec, J. Chroboczek, et al., Prebiotic role of softwood hemicellulose in healthy mice model, J. Funct. Foods 64 (2020) 103688, https://doi.org/10.1016/j.jff.2019.103688.

[3] D. Granato, D. Reshamwala, R. Korpinen, L. Azevedo, M.A.V. Carmo, T.M. Cruz, et al., From the forest to the plate – hemicelluloses, galactoglucomannan, glucuronoxylan, and phenolic-rich extracts from unconventional sources as functional food ingredients, Food Chem. 381 (2022) 132284, https://doi.org/10.1016/j.foodchem.2022.132284.

[4] J. Berglund, S. Azhar, M. Lawoko, M. Lindström, F. Vilaplana, J. Wohlert, et al., The structure of galactoglucomannan impacts the degradation under alkaline conditions, Cellulose 26 (2019) 2155–2175, https://doi.org/10.1007/s10570-018-1737-z.

[5] M. Bhattarai, L. Pitkänen, V. Kitunen, R. Korpinen, H. Ilvesniemi, P.O. Kilpeläinen, et al., Functionality of spruce galactoglucomannans in oil-in-water emulsions, Food Hydrocoll. 86 (2019) 154–161, https://doi.org/10.1016/j.foodhyd.2018.03.020.
[6] F. Valoppi, M.H. Lahtinen, M. Bhattarai, S.J. Kirjoranta, V.K. Juntti, L.J. Peltonen, et al., Centrifugal fractionation of softwood extracts improves the biorefinery workflow and yields functional emulsifiers, Green Chem. 21 (2019) 4691–4705, https://doi.org/10.1039/C9GC02007A.
[7] A. Esmeeta, S. Adhikary, V. Dharshnaa, P. Swarnamughi, Z.U. Maqsummiya, A. Banerjee, et al., Plant-derived bioactive compounds in colon cancer treatment: an updated review, Biomed. Pharmacother. 153 (2022) 113384, https://doi.org/10.1016/j.biopha.2022.113384.
[8] Y. Konkol, H. Vuorikoski, J. Tuomela, B. Holmbom, J. Bernoulli, Galactoglucomannan-rich hemicellulose extract from Norway spruce (Picea abies) exerts beneficial effects on chronic prostatic inflammation and lower urinary tract symptoms in vivo, Int. J. Biol. Macromol. 101 (2017) 222–229, https://doi.org/10.1016/j.ijbiomac.2017.03.079.
[9] A. Burgos-Edwards, A. Fernández-Romero, M. Carmona, I. Thuissard-Vasallo, G. Schmeda-Hirschmann, M. Larrosa, Effects of gastrointestinal digested polyphenolic enriched extracts of Chilean currants (Ribes magellanicum and Ribes punctatum) on *in vitro* fecal microbiota, Food Res. Int. 129 (2020) 108848, https://doi.org/10.1016/j.foodres.2019.108848.
[10] G.R. Caponio, M. Noviello, F.M. Calabrese, G. Gambacorta, G. Giannelli, M. De Angelis, Effects of grape pomace polyphenols and in vitro gastrointestinal digestion on antimicrobial activity: recovery of bioactive compounds, Antioxidants 11 (2022) 567, https://doi.org/10.3390/antiox11030567.
[11] M. Caban, U. Lewandowska, Encapsulation of polyphenolic compounds based on hemicelluloses to enhance treatment of inflammatory bowel diseases and colorectal cancer, Molecules 28 (2023) 4189, https://doi.org/10.3390/molecules28104189.
[12] A.S. Lima, R.D. Novaes, L.C. Pinheiro, L.A. de Almeida, H.S.D. Martino, A. Giusti-Paiva, et al., From waste to the gut: can blackcurrant press cake be a new functional ingredient? Insights on in vivo microbiota modulation, oxidative stress, and inflammation, Food Res. Int. 170 (2023) 112917, https://doi.org/10.1016/j.foodres.2023.112917.
[13] A. Brodkorb, L. Egger, M. Alminger, P. Alvito, R. Assunção, S. Ballance, et al., INFOGEST static in vitro simulation of gastrointestinal food digestion, Nat. Protoc. 14 (2019) 991–1014, https://doi.org/10.1038/s41596-018-0119-1.
[14] T.M. Cruz, A.S. Lima, A.O. Silva, N. Mohammadi, L. Zhang, L. Azevedo, et al., High-throughput synchronous erythrocyte cellular antioxidant activity and protection screening of phenolic-rich extracts: protocol validation and applications, Food Chem. 440 (2024) 138281, https://doi.org/10.1016/j.foodchem.2023.138281.
[15] A.S. Lima, V.G. Maltarollo, M.A.V. do Carmo, L.C. Pinheiro, T.M. Cruz, F.A.R. de Barros, et al., Blackcurrant press cake by-product: increased chemical bioaccessibility and reduced antioxidant protection after in vitro simulation of gastrointestinal digestion, Food Res. Int. 182 (2024) 114099, https://doi.org/10.1016/j.foodres.2024.114099.
[16] M.A.V. do Carmo, M. Fidelis, P.F. de Oliveira, L.Q. Feitoza, M.J. Marques, E. B. Ferreira, et al., Ellagitannins from jabuticaba (Myrciaria Jaboticaba) seeds attenuated inflammation, oxidative stress, aberrant crypt foci, and modulated gut microbiota in rats with 1,2 dimethyl hydrazine-induced colon carcinogenesis, Food Chem. Toxicol. 154 (2021) 112287, https://doi.org/10.1016/j.fct.2021.112287.
[17] R.P. Bird, Role of aberrant crypt foci in understanding the pathogenesis of colon cancer, Cancer Lett. 93 (1995) 55–71, https://doi.org/10.1016/0304-3835(95)03788-X.
[18] P.L. Sequetto, T.T. Oliveira, I.A.C. Soares, I.R.S.C. Maldonado, V.J. Mello, V. R. Pizziolo, et al., The flavonoid chrysin attenuates colorectal pathological remodeling reducing the number and severity of pre-neoplastic lesions in rats exposed to the carcinogen 1,2-dimethylhydrazine, Cell Tissue Res. 352 (2013) 327–339, https://doi.org/10.1007/s00441-013-1562-5.
[19] R.D. Novaes, P.L. Sequetto, R.V. Gonçalves, M.C. Cupertino, E.C. Santos, V. J. Mello, et al., Depletion of enteroendocrine and mucus-secreting cells is associated with colorectal carcinogenesis severity and impaired intestinal motility in rats, Microsc. Res. Tech. 79 (2016) 3–13, https://doi.org/10.1002/jemt.22534.
[20] A.B. Santana, B.S. Souto, N.C. Santos, J.A. Pereira, C.A. Tagliati, R.D. Novaes, et al., Murine response to the opportunistic bacterium Pseudomonas aeruginosa infection in gut dysbiosis caused by 5-fluorouracil chemotherapy-induced mucositis, Life Sci. 307 (2022) 120890, https://doi.org/10.1016/j.lfs.2022.120890.
[21] Y. Hu, Q. Lin, H. Zhao, X. Li, S. Sang, D.J. McClements, et al., Bioaccessibility and bioavailability of phytochemicals: influencing factors, improvements, and evaluations, Food Hydrocoll. 135 (2023) 108165, https://doi.org/10.1016/j.foodhyd.2022.108165.
[22] K.S. Mikkonen, S. Kirjoranta, C. Xu, J. Hemming, A. Pranovich, M. Bhattarai, et al., Environmentally compatible alkyd paints stabilized by wood hemicelluloses, Ind. Crop. Prod. 133 (2019) 212–220, https://doi.org/10.1016/j.indcrop.2019.03.017.
[23] V. Núñez-Gómez, R. González-Barrio, M.J. Periago, Interaction between dietary fibre and bioactive compounds in plant by-products: impact on bioaccessibility and bioavailability, Antioxidants 12 (2023) 976, https://doi.org/10.3390/antiox12040976.
[24] A. Niedzwiecki, M. Roomi, T. Kalinovsky, M. Rath, Anticancer efficacy of polyphenols and their combinations, Nutrients 8 (2016) 552, https://doi.org/10.3390/nu8090552.
[25] M.A.V. do Carmo, D. Granato, L. Azevedo, Chapter seven: antioxidant/pro-oxidant and antiproliferative activities of phenolic-rich foods and extracts: a cell-based point of view, Adv. Food Nutr. Res. (2021) 1–28, https://doi.org/10.1016/bs.afnr.2021.02.010.
[26] P. Ferreira-Santos, Z. Genisheva, C. Botelho, J. Santos, C. Ramos, J.Á. Teixeira, et al., Unravelling the biological potential of Pinus pinaster bark extracts, Antioxidants 9 (2020) 334, https://doi.org/10.3390/antiox9040334.
[27] G.U. Anywar, E. Kakudidi, H. Oryem-Origa, A. Schubert, C. Jassoy, Cytotoxicity of medicinal plant species used by traditional healers in treating people suffering from HIV/AIDS in Uganda, Front. Toxicol. 4 (2022) 832780, https://doi.org/10.3389/ftox.2022.832780.
[28] H. Corrigan, A. Dunne, N. Purcell, Y. Guo, K. Wang, H. Xuan, et al., Conceptual functional-by-design optimisation of the antioxidant capacity of trans-resveratrol, quercetin, and chlorogenic acid: application in a functional tea, Food Chem. 428 (2023) 136764, https://doi.org/10.1016/j.foodchem.2023.136764.
[29] K. Venkatachalam, R. Vinayagam, M. Arokia, V. Anand, N.M. Isa, R. Ponnaiyan, Biochemical and molecular aspects of 1,2-dimethylhydrazine (DMH)-induced colon carcinogenesis: a review, Toxicol. Res. 9 (2020) 2–18, https://doi.org/10.1093/toxres/tfaa004.
[30] C.W. Lee, H.J. Chen, G.R. Xie, C.K. Shih, Djulis (Chenopodium formosanum) prevents colon carcinogenesis via regulating antioxidative and apoptotic pathways in rats, Nutrients 11 (2019) 2168, https://doi.org/10.3390/nu11092168.
[31] Y. Wang, H.Y. Jin, M.Z. Fang, X.F. Wang, H. Chen, S.L. Huang, et al., Epigallocatechin gallate inhibits dimethylhydrazine-induced colorectal cancer in rats, World J. Gastroenterol. 26 (2020) 2064–2081, https://doi.org/10.3748/wjg.v26.i17.2064.
[32] B. Rackerby, H.J. Kim, D.C. Dallas, S.H. Park, Understanding the effects of dietary components on the gut microbiome and human health, Food Sci. Biotechnol. 29 (2020) 1463–1474, https://doi.org/10.1007/s10068-020-00811-w.
[33] V.S. Duarte, B.C.S. Cruz, R.S. Dias, L.P.D. Moreira, W.J.F.L. Junior, et al., Chemoprevention of DMH-induced early colon carcinogenesis in male BALB/c mice by administration of Lactobacillus paracasei DTA81, Microorganisms 8 (2020) 1994, https://doi.org/10.3390/microorganisms8121994.
[34] Y. Gamallat, X. Ren, W. Walana, A. Meyiah, R. Xinxiu, Y. Zhu, et al., Probiotic Lactobacillus rhamnosus modulates the gut microbiome composition attenuates preneoplastic colorectal Aberrant crypt foci, J. Funct. Foods 53 (2019) 146–156, https://doi.org/10.1016/j.jff.2018.12.018.